Electronic Journal of Biotechnology 77 (2025) 59–65

Contents lists available at ScienceDirect

Electronic Journal of Biotechnology

journal homepage: www.elsevier.com/locate/ejbt

Research article

Isolation, purification and physicochemical characterization of *Cichorium intybus* L. root polysaccharide and its protective effect against CCl_4-induced liver injury ☆

Yingze Ma, Zhiping Yang, Weili Huang *

Department of Digestive Medicine, Affiliated Hospital of Beihua University, Jilin, China

GRAPHICAL ABSTRACT

Isolation, purification and physicochemical characterization of *Cichorium intybus* L. root polysaccharide and its protective effect against CCl_4-induced liver injury

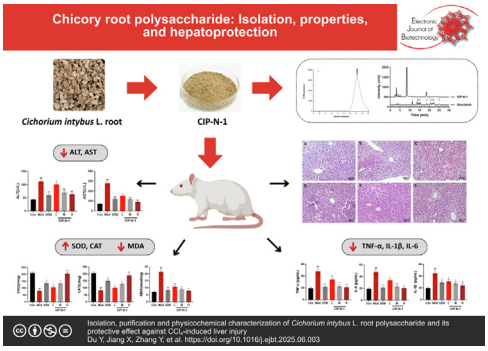

ARTICLE INFO

Article history:
Received 7 February 2025
Accepted 2 June 2025
Available online 19 August 2025

Keywords:
Anti-inflammatory
Antioxidant
Bioactive polysaccharides
Cichorium intybus L.
Hepatic diseases

ABSTRACT

Background: Liver injury is a major cause of hepatic diseases, often leading to impaired liver function. Current treatments face limitations due to potential hepatotoxicity, driving interest in alternative therapies like Traditional Chinese Medicine (TCM). *Cichorium intybus* L., a medicinal herb rich in bioactive polysaccharides, has shown promise in liver protection.
Results: A water-soluble polysaccharide (CIP-N-1), with an average molecular weight of 2.3 kDa, was isolated and purified from the water extract of *Cichorium intybus* L. root using DEAE cellulose column chromatography and CL-6B agarose gel chromatography. CIP-N-1 consists of 98.16% neutral sugars and 1.69% proteins, with its primary components being mannose and glucose in a ratio of 4.9:95.1. In vivo studies demonstrated CIP-N-1′s hepatoprotective effects by enhancing antioxidant activity, inhibiting lipid peroxidation, and reducing inflammation in CCl_4-induced liver injury.

☆ Audio abstract available in Supplementary material.

Peer review under responsibility of Pontificia Universidad Católica de Valparaíso.

* Corresponding author.
E-mail address: weili-huang@163.com (W. Huang).

https://doi.org/10.1016/j.ejbt.2025.06.003

Hepatic injury prevention
Hepatoprotective activity
Liver injury
Medicinal herb
Protective effect
Root polysaccharide

Conclusions: CIP-N-1 shows potential as a dietary supplement for alleviating chemical liver damage. Its antioxidant and anti-inflammatory properties support its use in liver health, offering a natural therapeutic option for hepatic injury prevention and treatment.

How to cite: Ma Y, Yang Z, Huang W. Isolation, purification and physicochemical characterization of *Cichorium intybus* L. root polysaccharide and its protective effect against CCl4-induced liver injury. Electron J Biotechnol 2025;77. https://doi.org/10.1016/j.ejbt.2025.06.003.

1. Introduction

Liver injury is a prevalent etiology underlying the development of numerous hepatic diseases and is consistently associated with them [1]. Hepatic damage compromises normal physiological processes, including the body's handling of exogenous substances, leading to progressive liver dysfunction [2,3]. The liver's role in metabolism renders it susceptible to harmful substances that can disrupt cellular function and trigger alterations in signaling pathways, culminating in apoptosis or necrosis [4,5]. Current pharmacotherapies for liver diseases are limited by potential hepatotoxic components. Traditional Chinese medicine (TCM) offers a promising alternative with minimal side effects, demonstrating significant improvements in liver antioxidant levels and tissue repair [6]. Various TCM ingredients have demonstrated efficacy in treating hepatic disorders. Given the escalating global health burden of liver injury, the development of dietary supplements aimed at mitigating chemical-induced liver damage is increasingly pertinent for reducing disease incidence [7,8,9,10].

Cichorium intybus L., a perennial herb from the Cichoridae family, is primarily found in Europe, Asia, and North Africa. This versatile plant is not only a popular culinary vegetable, suitable for cold dishes and salads, but also a widely utilized medicinal herb throughout history by ancient Greeks, Romans, and Chinese. In traditional Chinese medicine, *C. intybus* is known for its hepatoprotective, choleretic, stomachic, appetite-suppressing, diuretic, and anti-inflammatory properties, treating conditions such as jaundice, stomachache, poor appetite, edema, and oliguria [11,12,13]. Contemporary pharmacological research has confirmed *C. intybus*'s therapeutic potential for hepatitis, cholecystitis, and other diseases, along with its hypoglycemic, hypolipidemic, antioxidant, immunomodulatory, and antibacterial effects [14,15,16,17,18,19]. The plant contains a variety of bioactive substances, including sugars, terpenes, flavonoids, phenolic acids, and phenylpropanoids [20,21,22]. Notably, *C. intybus* polysaccharides are key active components with diverse biological activities, such as liver protection, blood glucose reduction, lipid-lowering, antitumor, anti-aging, anti-fatigue, and the promotion of calcium and phosphorus absorption [17,23]. This study extracted, isolated, and purified a polysaccharide from *C. intybus* roots and examined its protective effects against CCl_4-induced liver injury in mice, offering experimental support for the development of *C. intybus* polysaccharide-based dietary supplements and therapeutic agents for preventing and treating hepatic damage.

2. Materials and methods

2.1. Materials and reagents

The roots of *C. intybus* were procured from Jilin Sanzhentang Canrong Co., Ltd., located in Jilin City, Jilin Province, China, and authenticated by Senior Pharmacist Yinglan Jin of the Jilin Food and Drug Inspection Institute, adhering to the standards outlined in the Pharmacopoeia of the People's Republic of China (PPRC-2020).

A range of dextran standards with varying molecular weights and monosaccharide standards (d-Man, Rha, d-GluA, d-GalA, d-Glu, d-Gal, d-Ara, d-Xyl, d-Fuc), along with 3-(4,5-dimethylthiazol-2-yl)-2,5-diphenyltetrazolium bromide (MTT) and trifluoroacetic acid (TFA), were acquired from Sigma Chemical Co. (St. Louis, MO, USA). Additionally, DEAE-cellulose-52, Sepharose CL-6B, and Sephadex G100 were purchased from GE Healthcare (Chicago, Illinois, USA). All other chemicals and reagents utilized in the study were of analytical grade. Commercial ELISA kits for TNF-α, IL-1β, and IL-6 were obtained from Langdun Biotechnology Co., Ltd., while AST, ALT, SOD, CAT, and MDA kits were acquired from Nanjing Jiancheng Bioengineering Institute.

2.2. Extraction and purification of the polysaccharide

Crude polysaccharide extraction was adapted from a protocol described by Song et al. [24]. Briefly, 1000 g of dried *C. intybus* root powder was refluxed with 5 L of absolute ethanol at 80°C for 4 h to remove pigments, lipids, and other small molecules, following the method of Yuan et al. [25]. The ethanol-insoluble residue (768 g) was then re-extracted four times with 10 L of distilled water at 90°C for 2 h each. After centrifugation at 3500 rpm for 10 min, the supernatants were pooled, mixed with four volumes of absolute ethanol, vigorously agitated, and incubated overnight at 4°C to precipitate polysaccharides. The precipitate was redissolved in distilled water (5%, w/v), and proteins were removed using the Sevag method [26]. The aqueous phase was dialyzed against a 3500 Da molecular weight cutoff membrane for 72 h. The dialyzed solution was collected, freeze-dried, and yielded 56.3 g of crude *C. intybus* polysaccharides (CIPs).

Ten grams of CIPs were dissolved in 20 mL of distilled water, filtered through a 5 μm filter, and loaded onto a DEAE-cellulose-52 column (2.6 × 40.0 cm). The column was first eluted with 2 L of distilled water. The eluate was collected, concentrated, and freeze-dried to yield a neutral polysaccharide fraction (CIP-N, 2.26 g) and two acidic fractions (CIP-A, 1.82 g; CIP-B, 0.89 g). Further purification of CIP-N was performed using a Sepharose CL-6B column (2 × 100 cm) with distilled water as the mobile phase. The major polysaccharide fraction was concentrated and freeze-dried to afford a white, fluffy pure polysaccharide (CIP-N-1, 1.33 g). Purity was assessed using the phenol–sulfuric acid method [27] and UV–vis spectroscopy. CIP-N-1 was dissolved in distilled water at 0.1 mg/mL, and its UV–vis absorption spectrum was recorded from 200 to 350 nm using a Cary 5000 UV–vis spectrophotometer (Varian, USA). This procedure was reiterated until the desired quantity of CIP-N-1 was obtained for subsequent experiments. The prepared CIP-N-1 was then freeze-dried for storage.

2.3. Molecular weight determination

An adequate amount of CIP-N-1 polysaccharide was dissolved in 0.2 M NaCl to a concentration of 5 mg/mL. After complete dissolution, the solution was filtered through a 0.22 μm filter to remove any suspended particles, ensuring accurate chromatographic analysis. Subsequently, 20 μL of the polysaccharide solution was sub-

jected to High-Performance Gel Permeation Chromatography (HPGPC) using a Shimadzu LC-20AT system with an RID-20A detector. Analysis was performed on a TSK Gel G-4000PWXL column (7.8 × 300 mm) at a column temperature of 40°C, with 0.2 M NaCl as the mobile phase and a flow rate of 0.6 mL/min.

To ascertain the molecular weight of polysaccharides, a standard curve was generated using glucose polymers with known molecular weights of 1 kDa, 5 kDa, 12 kDa, 25 kDa, and 50 kDa. This curve was established by calibrating and quantifying the standard substances. During analysis, the molecular weight of the sample polysaccharide was accurately determined by aligning its chromatographic peaks with those of the standard curve, facilitating precise molecular weight estimation [28].

2.4. Monosaccharide composition analysis

Accurately weigh CIP-N-1 and dissolve it in a 2 M hydrochloric acid–methanol solution to prepare a 2 mg/mL sample solution, ensuring complete dissolution for a homogeneous sample. Introduce nitrogen gas and incubate the solution in an 80°C constant-temperature metal bath for 16 h to facilitate hydrolysis. The choice of hydrolysis conditions is critical for optimizing efficiency. Post-hydrolysis, use a nitrogen blower to remove residual hydrochloric acid–methanol, ensuring product purity. Transfer the product to a 2 M trifluoroacetic acid (TFA) environment and heat at 120°C for 1 h to enhance transformation and reaction rate. Complete the drying process to eliminate moisture, solvent residues and obtain a dry, pure product.

To improve detection sensitivity and stability, the target product underwent pre-column derivatization with 1-phenyl-3-methyl-5-pyrazolone (PMP). The sample was then filtered through a 0.22 μm membrane to remove any small particles and impurities. The analysis utilized a Shimadzu HPLC system, featuring an LC-20AT pump and an SPD-20A UV–Vis detector, coupled with a COSMOSIL 5C18-PAQ column (4.6 mm × 250 mm). The mobile phase consisted of 80.8% phosphate-buffered saline (PBS, 0.1 M, pH 7.0) and 19.2% acetonitrile (v′/v), mixed in a 1:3 ratio, to optimize target product detection [29].

2.5. Protective effect of CIP-N-1 against CCl_4-induced liver injury in mice

2.5.1. Animal handling

Following a three-day acclimation period, ninety ICR male mice were randomly assigned to six groups: a blank control group (Con), a model group (Mod), a positive drug group (DDB, biphenyl diester 200 mg/kg/d), and three CIP-N-1 dosage groups (L: 100 mg/kg/d, M: 200 mg/kg/d, H: 400 mg/kg/d). Mice in the Con and Mod groups received daily gavage with an equivalent volume of normal saline, and on the 10th day, an equal volume of physiological saline was administered intraperitoneally 4 h post-gavage. In contrast, mice in the other groups were injected intraperitoneally with 0.1% CCl_4 in peanut oil. After 24 h, blood samples were collected from the orbital venous plexus, centrifuged at 12,000 rpm for 10 min to obtain serum. Mice were then euthanized by cervical dislocation, and their livers were excised, weighed, and utilized for calculating the liver index and assessing biochemical indicators.

2.5.2. Liver index

Prior to treatment initiation, the body weight of the mice was measured and recorded. Body weight and liver weight were also noted immediately before sacrifice. The liver index was subsequently calculated using the formula:

$$\text{Liver index} = \text{Liver weight (g)}/\text{body weight (g)} \times 100\%$$

2.5.3. Detection of serum ALT and AST levels in mice

Serum levels of aspartate aminotransferase (AST) and alanine aminotransferase (ALT) in mice were assayed using a fully automated biochemical analyzer, adhering to the manufacturer's instructions.

2.5.4. Detection of SOD activity and MDA content in the liver tissue of mice

Mouse liver tissue was homogenized to a 10% suspension. The activities of malondialdehyde (MDA) and the concentrations of superoxide dismutase (SOD) within the suspension were then measured following the instructions provided with the kits.

2.5.5. Detection of TNF-α, IL-6 and IL-1β contents in the serum of mice

The serum concentrations of tumor necrosis factor-alpha (TNF-α), interleukin-6 (IL-6), and interleukin-1 beta (IL-1β) in mice were determined using an enzyme-linked immunosorbent assay (ELISA).

2.5.6. Pathomorphological observation on the liver tissue of mice by HE staining

Liver tissue sections, preserved at 4°C, were retrieved and allowed to equilibrate at room temperature for 20 min. After drying, sections were washed thrice with phosphate-buffered saline (PBS), 3 min each. Hematoxylin staining was applied for 5 min, followed by PBS rinses to remove excess dye. Sections were differentiated in a 75% alcohol-hydrochloric acid solution (1%) for 20 s and washed with PBS for 1 min. Blue color was restored with dilute ammonia water for 30 s, followed by PBS washes (1 min each) and a final rinse. Eosin staining was conducted for 20–30 s, followed by PBS rinses and three 2-min rinses. Ethanol gradients dehydrated the sections, and xylene I and II were used for 5 min each to improve transparency. Sections were mounted with neutral gum and air-dried. Pathological changes in mouse liver tissue were examined at 200 × magnification using an optical microscope.

2.6. Data processing

Data analysis was performed using SPSS 19.0 software, with results expressed as mean ± standard deviation (standard error). Intergroup comparisons were conducted using the Student's *t*-test, and a $p < 0.05$ was deemed statistically significant.

3. Results

3.1. Purification and characterization of CIP-N-1

After water extraction and alcohol precipitation, crude *C. intybus* polysaccharides (CIPs) from *C. intybus* roots were obtained with a 5.63% yield. Subsequently, CIPs were subjected to gradient elution using DEAE cellulose ion exchange column chromatography, yielding a neutral polysaccharide fraction (CIP-N) at 22.6%, as well as acidic fractions (CIP-A and CIP-B) with yields of 18.2% and 8.9%, respectively. Fraction CIP-A was further separated using Sepharose CL-6B, resulting in three distinct elution peaks. The main elution peak's eluents were collected, freeze-dried, and yielded a fraction, CIP-N-1, accounting for 58.8% of CIP-N. The overall yield of CIP-N-1 represented 0.75% of the *C. intybus* root mass. By repeating the above steps, we obtained a total of 7.28 g of CIP-N-1.

The characteristics of CIP-N-1, including neutral sugar, uronic acid, protein, sulfate content, molecular weight, and monosaccharide composition, are presented in Table 1. The GPC chromatogram of CIP-N-1 displayed a single, symmetrical, sharp peak (Fig. 1), suggesting its homogeneity as a polysaccharide. HPLC analysis determined the monosaccharide composition of CIP-N-1, revealing a

Table 1
Chemical composition, molecular weight and monosaccharide composition of CIP-N-1.

Yield (%)	Molecular weight (KD)	Neutral sugar (%)	Uronic acid (%)	Protein (%)	Sulfate (%)	Sugar components (mol%)	
						Man	Glc
0.75	2.3	98.16	nd	1.69	nd	4.9	95.1

nd: not detected.

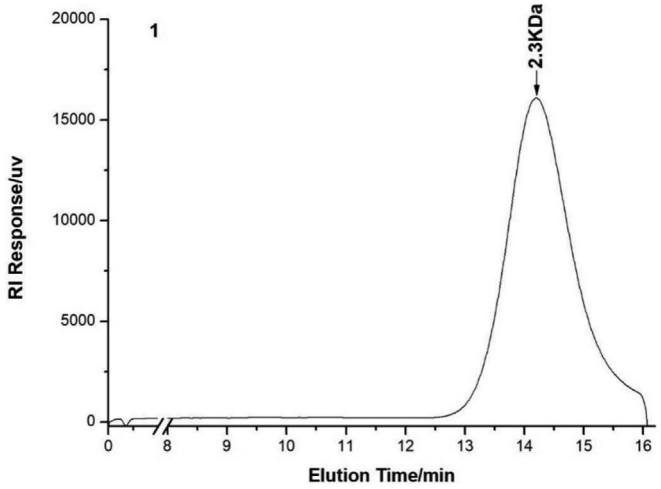

Fig. 1. Elution curve of CIP-N-1 in HPGPC.

molar ratio of mannose and glucose at 4.9 and 95.1, respectively. Consequently, CIP-N-1 could be considered a novel heteropolysaccharide derived from *C. intybus* roots (Fig. 2).

3.2. Effects of CIP-N-1 on liver index in mice

As depicted in Fig. 3, the liver index of mice in the Mod group was significantly elevated compared to the Con group ($p < 0.01$), indicating potential liver swelling due to CCl_4-induced inflammation. The liver indices of mice treated with low (L-), medium (M-), and high (H-) doses of CIP-N-1 were significantly lower than that of the Mod group ($p < 0.05$), suggesting that CIP-N-1 can suppress the inflammatory response caused by CCl_4.

3.3. Effects of CIP-N-1 on serum ALT and AST activities in mice

Fig. 4 illustrates that serum levels of ALT and AST were significantly higher in the Mod group than in the Con group ($p < 0.05$, $p < 0.01$), indicating significant liver damage and confirming the model's success. In comparison, L-, M-, and H-CIP-N-1 treated

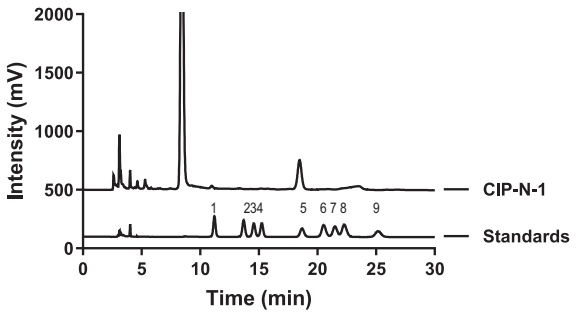

Fig. 2. Chromatograms of nine PMP-derivative monosaccharide standards and CIP-N-1. 1: Man, 2: GlcA, 3: Rha, 4: GalA, 5: Glc, 6: Gal, 7: Xyl, 8: Ara, and 9: Fuc.

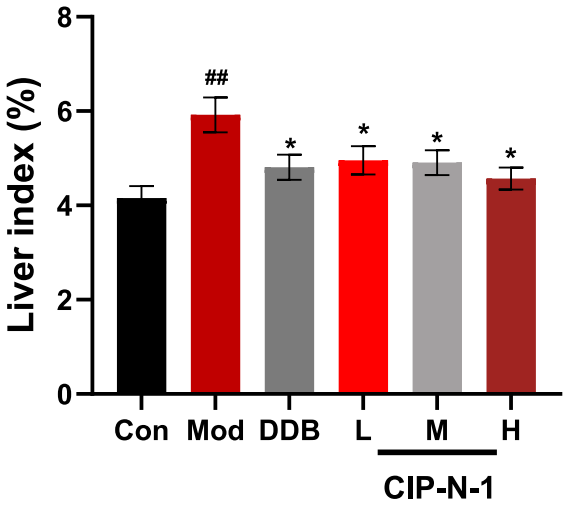

Fig. 3. Effects of CIP-N-1 on liver index of mice induced by CCl_4 (n = 15). Con: blank control group; Mod: model group; DDB: positive drug group; L: low-dose CIP-N-1 group; M: medium-dose CIP-N-1 group; H: high-dose CIP-N-1 group. Compared with the Con group, $^{\#\#}p < 0.01$; compared with the Mod group, $^{*}p < 0.05$, $^{**}p < 0.01$.

groups exhibited significantly reduced serum ALT and AST activities compared to the Mod group ($p < 0.01$, $p < 0.05$).

3.4. Effects of CIP-N-1 on the antioxidant enzyme activities in mice

In this study, the impact of CIP-N-1 on hepatic oxidative stress in mice was assessed by evaluating the activities of two key antioxidant enzymes, superoxide dismutase (SOD) and catalase (CAT), as well as the concentration of a lipid peroxidation marker, malondialdehyde (MDA), in liver tissue. As illustrated in Fig. 5, the antioxidant system balance in the Mod group was markedly disturbed relative to the Con group, evidenced by reduced SOD and CAT activities ($p < 0.01$) and elevated MDA levels in the liver ($p < 0.01$). In comparison to the Mod group, the liver tissues of mice in the H-, M-, and L-CIP-N-1 groups exhibited significant enhancements in SOD and CAT activities ($p < 0.05$, $p < 0.01$), along with decreased MDA content ($p < 0.01$). These findings suggest that CIP-N-1 has the potential to mitigate oxidative stress-induced damage and suppress lipid peroxidation in the mouse liver.

3.5. Effects of CIP-N-1 on the inflammatory factors level in mice

To elucidate the anti-inflammatory mechanisms of CIP-N-1, an enzyme-linked immunosorbent assay (ELISA) was employed to measure the serum levels of tumor necrosis factor-alpha (TNF-α), interleukin-6 (IL-6), and interleukin-1 beta (IL-1β) in mice. As depicted in Fig. 6, the serum concentrations of TNF-α, IL-6, and IL-1β were significantly elevated in the Mod group compared to the Con group ($p < 0.01$), signifying that CCl_4 induced inflammatory damage. However, treatment with CIP-N-1 led to a significant reduction in the levels of TNF-α, IL-6, and IL-1β ($p < 0.05$, $p < 0.01$), suggesting that CIP-N-1 can ameliorate CCl_4-induced hepatic inflammation in mice.

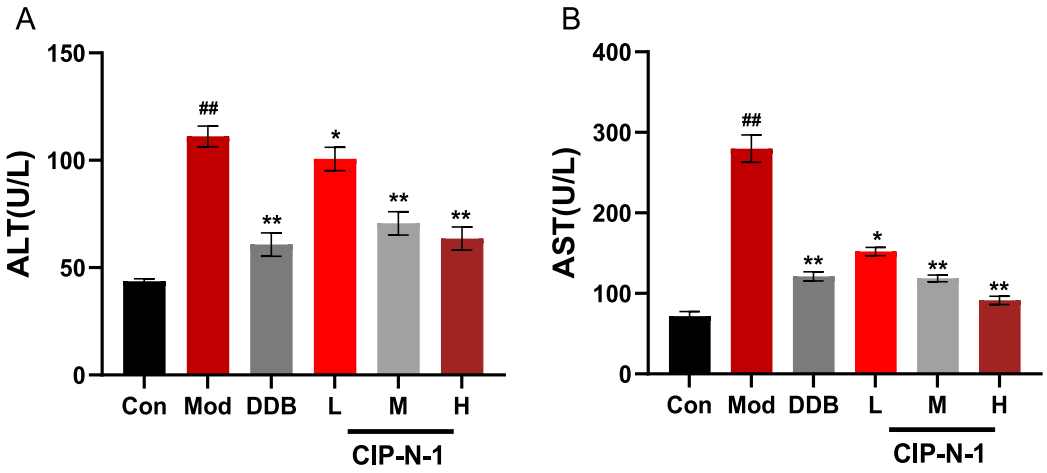

Fig. 4. Effects of CIP-N-1 on serum ALT and AST activities of mice induced by CCl_4 (n = 15). (A) ALT and (B) AST. Con: blank control group; Mod: model group; DDB: positive drug group; L: low-dose CIP-N-1 group; M: medium-dose CIP-N-1 group; H: high-dose CIP-N-1 group. Compared with the Con group, $^{\#\#}p < 0.01$; compared with the Mod group, $^{*}p < 0.05$, $^{**}p < 0.01$.

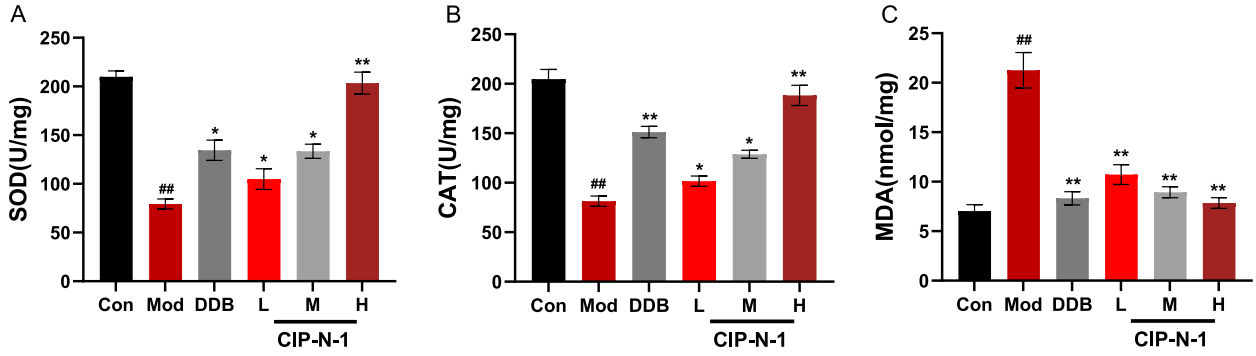

Fig. 5. Effects of CIP-N-1 on liver tissue SOD activity, CAT activity and MDA content of mice induced by CCl_4 (n = 15). (A) SOD, (B) CAT and (C) MDA. Con: blank control group; Mod: model group; DDB: positive drug group; L: low-dose CIP-N-1 group; M: medium-dose CIP-N-1 group; H: high-dose CIP-N-1 group. Compared with the Con group, $^{\#\#}p < 0.01$; compared with the Mod group, $^{*}p < 0.05$, $^{**}p < 0.01$.

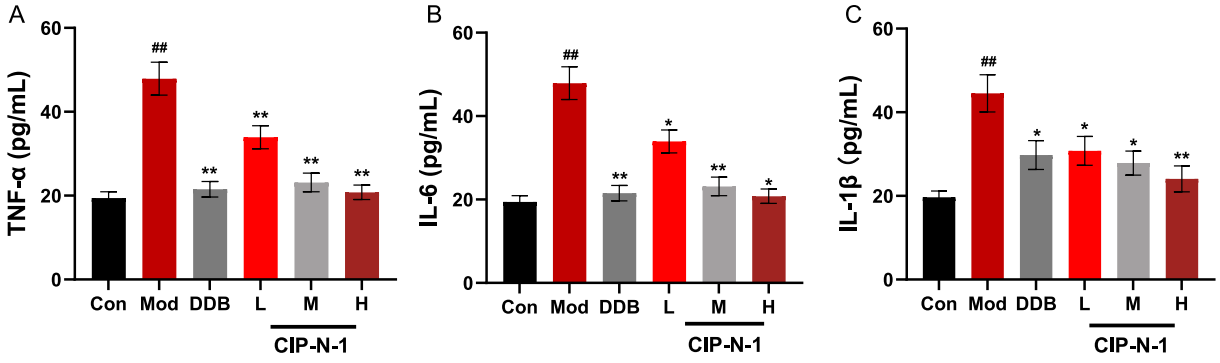

Fig. 6. Effects of CIP-N-1 on serum TNF-α, IL-6 and IL-1β levels of mice induced by CCl_4 (n = 15). (A) TNF-α, (B) IL-6 and (C) IL-1β. Con: blank control group; Mod: model group; DDB: positive drug group; L: low-dose CIP-N-1 group; M: medium-dose CIP-N-1 group; H: high-dose CIP-N-1 group. Compared with the Con group, $^{\#\#}p < 0.01$; compared with the Mod group, $^{*}p < 0.05$, $^{**}p < 0.01$.

3.6. Pathomorphological observation of mouse liver tissue

The hematoxylin and eosin (HE) staining findings (Fig. 7) revealed that the liver cells in the Con group were distinct and well-preserved, with the nucleus positioned centrally and the hepatic lobular structure remaining intact, devoid of inflammatory cell infiltration in the portal areas. Conversely, in the Mod group, hepatic lobules exhibited damage, cellular disorganization, necrosis, and inflammatory cell infiltration near the central vein. Following the administration of CIP-N-1, there was a notable restoration of liver cell architecture, a decrease in the severity of lesions, a reduction in necrotic areas, and an enhancement in cell morphology.

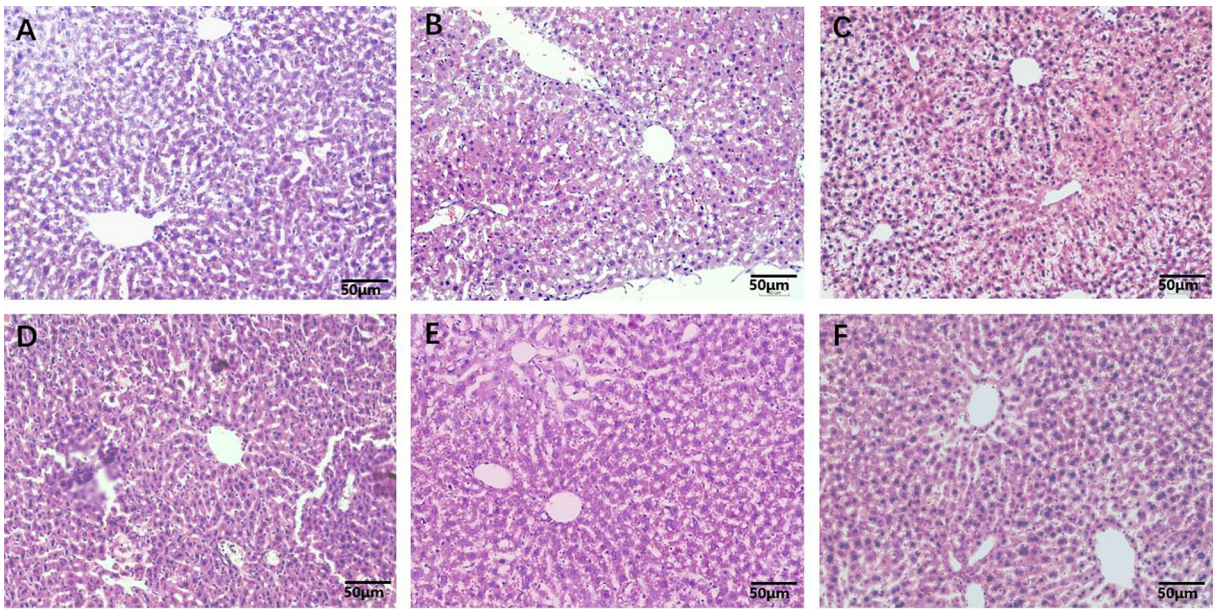

Fig. 7. Pathomorphological observation on the liver tissue of mice. (200×, n = 5). (A) Con: blank control group, (B) Mod: model group, (C) DDB: positive drug group, (D) L: low-dose CIP-N-1 group, (E) M: medium-dose CIP-N-1 group, (F) H: high-dose CIP-N-1 group.

4. Discussion

Carbon tetrachloride (CCl_4) is a widely used agent for creating animal models of liver injury, producing pathophysiological symptoms analogous to those seen in human hepatic disorders [30,31]. Over several decades, it has been employed to assess the anti-hepatotoxic or hepatoprotective potential of various natural substances. Serum ALT is a precise marker for liver cell integrity, while AST is sensitive to mitochondrial damage. Changes in ALT and AST levels indicate the severity of liver damage and recovery. Significant elevations in these enzymes confirm successful induction of liver injury.

It is well-established that CCl_4 is metabolized into highly reactive free radicals by cytochrome P450 enzymes, which react vigorously with oxygen (O_2) to increase free radical production [32]. Additionally, CCl_4 metabolites can react with polyunsaturated fatty acids, forming covalent bonds with lipids and proteins, initiating lipid peroxidation and cell membrane damage, ultimately causing hepatic injury [33]. Excessive free radicals stimulate macrophages in the liver to produce inflammatory mediators, leading to local inflammation [34]. This study measured various oxidation and inflammation-related indicators to provide a theoretical basis for subsequent mechanistic investigations.

The literature indicates that the primary structure, molecular weight, branching, and linkage type of natural polysaccharides play crucial roles in preserving their biological activity. In vivo experiments have demonstrated that CIP-N-1 exhibits biological activity. To investigate the structure–function relationship, a chemical analysis was conducted. The monosaccharide composition revealed that glucose is the predominant sugar in CIP-N-1, with minor amounts of mannose. Li et al. [35] reported that polysaccharides extracted from *Pleurotus ferulae* consisted of 97% glucose, followed by 3% mannose and galactose. Yuan et al. [25], Shi et al. [36] and Wang et al. [26] also noted that polysaccharides purified from *Polygonatum* primarily contained 98.1–98.3% glucose. Numerous studies have emphasized the importance of water solubility for maintaining the biological activity of polysaccharides, with the degree of branching directly influencing solubility. This is likely due to the larger contact surface area available for free radical scavenging in water-soluble polysaccharides. The water-soluble CIP-N-1, with its relatively high degree of branching, demonstrates superior biological activity.

5. Conclusions

In this study, a water-soluble polysaccharide, CIP-N-1, with a molecular weight of 2.3 kDa, was successfully isolated and purified from the root extract of Cichorium intybus L. using DEAE cellulose and CL-6B agarose gel chromatography. The structural characterization revealed a mannose-to-glucose molar ratio of 4.9:95.1. The key finding of this research is that CIP-N-1 exhibits significant hepatoprotective effects, as demonstrated by in vivo experiments, which showed enhanced antioxidant enzyme activity, inhibition of lipid peroxidation, and reduction of pro-inflammatory mediator activity, thereby effectively preventing chemical-induced liver injury. The potential benefits of using CIP-N-1 as a dietary supplement include its natural origin and excellent biocompatibility, making it a safe hepatoprotective agent. Its antioxidant and anti-inflammatory properties may contribute to improving liver health and preventing liver injury-related diseases. Furthermore, the potential applications of CIP-N-1 could extend to the management of other chronic diseases associated with oxidative stress and inflammation. These findings suggest that CIP-N-1 holds promise as a dietary supplement for preventing chemical-induced liver damage and may provide new directions for the development of functional foods or pharmaceuticals.

CRediT authorship contribution statement

Yingze Ma: Writing – original draft, Methodology, Formal analysis, Data curation, Conceptualization. **Zhiping Yang:** Visualization, Investigation, Formal analysis. **Weili Huang:** Writing – review & editing, Supervision, Project administration, Funding acquisition.

Ethical approval

All procedures were conducted in accordance with the guidelines for the care and use of laboratory animals (China).

Financial support

This work was financially supported by Science and Technology Research Project of the "13th Five-Year Plan" of the Education Department of Jilin Province (JJKH20190656KJ).

Declaration of competing interest

The authors declare that they have no known competing financial interests or personal relationships that could have appeared to influence the work reported in this paper.

Supplementary material

https://doi.org/10.1016/j.ejbt.2025.06.003.

Data availability

No data was used for the research described in the article.

References

[1] Zhang J, Yang Z, Liu X, et al. New insights into the pathogenesis of alcoholic liver disease based on global research. Dig Dis Sci 2025;70(3):903–18. https://doi.org/10.1007/s10620-024-08778-y. PMid: 39806089.
[2] Almalki WH, Almujri SS. Aging, ROS, and cellular senescence: A trilogy in the progression of liver fibrosis. Biogerontology 2024;26(1):10. https://doi.org/10.1007/s10522-024-10153-3. PMid: 39546058.
[3] Abreo Medina ADP, Shi M, Wang Y, et al. Exploring extracellular vesicles: A novel approach in nonalcoholic fatty liver disease. J Agric Food Chem 2025;73(5):2717–31. https://doi.org/10.1021/acs.jafc.4c09209. PMid: 39846785.
[4] Chodup P, Samodelov SL, Visentin M, et al. Drug-induced liver injury associated with emerging cancer therapies. Liver Int 2025;45(2):e70002. https://doi.org/10.1111/liv.70002. PMid: 39853863.
[5] Dara L, De Martin E. Immune-mediated liver injury from checkpoint inhibitor: An evolving frontier with emerging challenges. Liver Int 2025;45(2):e16198. https://doi.org/10.1111/liv.16198. PMid: 39868913.
[6] Li J, Chen Y, Zhang S, et al. Purslane (*Portulaca oleracea* L.) polysaccharide attenuates carbon tetrachloride-induced acute liver injury by modulating the gut microbiota in mice. Genomics 2025;117(1):110983. https://doi.org/10.1016/j.ygeno.2024.110983. PMid: 39734003.
[7] Pu X, Fu Y, Yang Y, et al. *Ginkgo biloba* extract alleviates CCl_4-induced acute liver injury by regulating PI3K/AKT signaling pathway. Heliyon 2024;10(4):e26093. https://doi.org/10.1016/j.heliyon.2024.e26093. PMid: 38390084.
[8] Hamidi M, Mirzaei R, Delattre C, et al. Characterization of a new exopolysaccharide produced by *Halorubrum* sp. TBZ112 and evaluation of its anti-proliferative effect on gastric cancer cells. 3 Biotech 2019;9(1):1. https://doi.org/10.1007/s13205-018-1515-5. PMid: 30555767.
[9] Gao LJ, Du BY, Ma QH, et al. Multiplex-PCR method application to identify duck blood and its adulterated varieties. Food Chem 2024;444:138673. https://doi.org/10.1016/j.foodchem.2024.138673. PMid: 38330615.
[10] Li HY, Xu GY, Zhu WH, et al. Editorial: Application of natural medicinal products in preventing and ameliorating aging-caused cognitive impairment. Front Pharmacol 2022;13:1059398. https://doi.org/10.3389/fphar.2022.1059398. PMid: 36408250.
[11] Abbasi BHA, Rashid N, Bilal RM, et al. Supplementation of *Cichorium intybus* roots improved the growth performance, immunity response, gut ecology and morphology of broilers chicken Ross308 strain. J King Saud Univ Sci 2024;36(8):103314. https://doi.org/10.1016/j.jksus.2024.103314.
[12] Afzal AH, Alam O, Zafar S, et al. Application of machine learning for the prediction of absorption, distribution, metabolism and excretion (ADME) properties from *Cichorium intybus* plant phytomolecules. Processes 2024;12(11):2488. https://doi.org/10.3390/pr12112488.
[13] Zheng T, Jing M, Gong T, et al. Deletion of the *yqeK* gene leads to the accumulation of Ap4A and reduced biofilm formation in *Streptococcus mutans*. Mol Oral Microbiol 2022;37(1):9–21. https://doi.org/10.1111/omi.12356. PMid: 34761536.
[14] Baria DM, Patel NY, Yagnik SM, et al. Exopolysaccharides from marine microbes with prowess for environment cleanup. Environ Sci Pollut Res Int 2022;29(51):76611–25. https://doi.org/10.1007/s11356-022-23198-z. PMid: 36166130.
[15] Aljumayi H. Antioxidant activities of chicory (*Cichorium intybus* L.) and purslane (*Portulaca oleracea* L.) leaves powder and their applications for preservation of cupcakes. Ital J Food Sci 2025;37(1):345–65. https://doi.org/10.15586/ijfs.v37i1.2790.
[16] Babenko AN, Krepkova LV, Borovkova MV, et al. Effects of chicory (*Cichorium intybus* L.) extract on male rat reproductive system, pregnancy and offspring development. Pharmaceuticals (Basel) 2024;17(6):700. https://doi.org/10.3390/ph17060700.
[17] Sun JH, Liu X, Cong LX, et al. Metabolomics study of the therapeutic mechanism of *Schisandra chinensis* lignans in diet-induced hyperlipidemia mice. Lipids Health Dis 2017;16(1):145. https://doi.org/10.1186/s12944-017-0533-3. PMid: 28764799.
[18] Cinar D, Altinoz E, Elbe H, et al. Therapeutic effect of melatonin on CCl_4-induced fibrotic liver model by modulating oxidative stress, inflammation, and TGF-β1 signaling pathway in pinealectomized rats. Inflammation 2025;48:1093–108. https://doi.org/10.1007/s10753-024-02101-7. PMid: 39007940.
[19] Sishu NK, Selvaraj CI. Phytochemistry, pharmacological applications, and therapeutic effects of green synthesized nanomaterials using *Cichorium* species-a comprehensive review. Naunyn Schmiedebergs Arch Pharmacol 2024;397(11):8527–59. https://doi.org/10.1007/s00210-024-03221-5. PMid: 38900250.
[20] Al-Salim KAR, Al-Charak AGH. GC-mass analysis of *Ginkgo biloba* and *Cichorium intybus* and their neuroprotective effects in a rat model of Alzheimer's disease. Int J Biomed 2024;14(3):510–5. https://doi.org/10.21103/Article14(3)_OA20.
[21] Feng YB, Li H, Chen C, et al. Study on the hepatoprotection of *Schisandra chinensis* caulis polysaccharides in nonalcoholic fatty liver disease in rats based on metabolomics. Front Pharmacol 2021;12:727636. https://doi.org/10.3389/fphar.2021.727636. PMid: 34621168.
[22] Li GD, Hayes RC, Gardner MJ, et al. Companion legume species for chicory in a phased farming system. Eur J Agron 2025;164:127488. https://doi.org/10.1016/j.eja.2024.127488.
[23] Yao C, Jiang N, Sun X, et al. Effects of inulin-type oligosaccharides (JSO) from *Cichorium intybus* L. on behavioral deficits induced by chronic restraint stress in mice and associated molecular alterations. Front Pharmacol 2024;15:1484337. https://doi.org/10.3389/fphar.2024.1484337. PMid: 39555096.
[24] Song J, Wu Y, Jiang G, et al. Sulfated polysaccharides from *Rhodiola sachalinensis* reduce d-gal-induced oxidative stress in NIH 3T3 cells. Int J Biol Macromol 2019;140:288–93. https://doi.org/10.1016/j.ijbiomac.2019.08.052. PMid: 31400419.
[25] Yuan G, Wang Y, Niu H, et al. Isolation, purification, and physicochemical characterization of *Polygonatum* polysaccharide and its protective effect against CCl_4-induced liver injury *via* Nrf2 and NF-κB signaling pathways. Int J Biol Macromol 2024;261(Pt-2). https://doi.org/10.1016/j.ijbiomac.2024.129863. PMid: 38307425.
[26] Wang Y, Niu H, Ma Y, et al. Isolation, purification, fractionation, and hepatoprotective activity of *Polygonatum* polysaccharides. Molecules 2024;29(5):1038. https://doi.org/10.3390/molecules29051038. PMid: 38474549.
[27] Li H, Xu G, Yuan G. Effects of an *Armillaria mellea* polysaccharide on learning and memory of D-galactose-induced aging mice. Front Pharmacol 2022;13:919920. https://doi.org/10.3389/fphar.2022.919920. PMid: 35924065.
[28] Niu J, Xu G, Jiang S, et al. *In vitro* antioxidant activities and anti-diabetic effect of a polysaccharide from *Schisandra sphenanthera* in rats with type 2 diabetes. Int J Biol Macromol 2017;94(Pt-A):154–60. https://doi.org/10.1016/j.ijbiomac.2016.10.015. PMid: 27720962.
[29] Bishnolia M, Yadav P, Singh SK, et al. Methyl donor ameliorates CCl_4-induced liver fibrosis by inhibiting inflammation, and fibrosis through the downregulation of EGFR and DNMT-1 expression. Food Chem Toxicol 2025;196:115230. https://doi.org/10.1016/j.fct.2024.115230. PMid: 39736447.
[30] Qin BF, Zhang JJ, Feng QY, et al. Specnuezhenide ameliorates hepatic fibrosis *via* regulating SIRT6-mediated inflammatory signaling cascades. J Ethnopharmacol 2024;335:118646. https://doi.org/10.1016/j.jep.2024.118646. PMid: 39097210.
[31] Cui L, Tan YJ, Xu SQ, et al. Ginsenoside Rd, a natural production for attenuating fibrogenesis and inflammation in hepatic fibrosis by regulating the ERRα-mediated P2X7r pathway. Food Funct 2023;14(12):5606–19. https://doi.org/10.1039/d3fo01315d. PMid: 37249244.
[32] Xu G, Lv X, Feng Y, et al. Study on the effect of active components of *Schisandra chinensis* on liver injury and its mechanisms in mice based on network pharmacology. Eur J Pharmacol 2021;910:174442. https://doi.org/10.1016/j.ejphar.2021.174442. PMid: 34492285.
[33] Sohail A, Shams F, Nawaz A, et al. Antifibrotic potential of reserpine (alkaloid) targeting Keap1/Nrf2; oxidative stress pathway in CCl_4-induced liver fibrosis. Chem Biol Interact 2025;407:111384. https://doi.org/10.1016/j.cbi.2025.111384. PMid: 39800144.
[34] Ni Q, Lin J, Huang W, et al. Kehuang capsule inhibits MAPK and AKT signaling pathways to mitigate CCl_4-induced acute liver injury. Liver Res 2024;8(4):269–81. https://doi.org/10.1016/j.livres.2024.11.006. PMid: 39958915.
[35] Li J, Aipire A, Zhao H, et al. *Pleurotus ferulae* polysaccharides improve the antitumor efficacy of therapeutic human papillomavirus dendritic cell-based vaccine. Hum Vaccin Immunother 2019;15(3):611–9. https://doi.org/10.1080/21645515.2018.1547604. PMid: 30427754.
[36] Shi L, Wang Y, Guan Y, et al. To establish a new quality assessment method based on the regulation of intestinal microbiota in type 2 diabetes by lignans of *Schisandra chinensis* (Turcz.) Baill. J Ethnopharmacol 2025;348. https://doi.org/10.1016/j.jep.2025.119822. PMid: 40250638.